PHYSICAL REVIEW D **81,** 056006 (2010)

Analysis of the $\Lambda_b \to \Lambda l^+ l^-$ decay in QCD

T. M. Aliev,[1,*,†] K. Azizi,[2,‡] and M. Savci[1,§]

[1]*Physics Department, Middle East Technical University, 06531 Ankara, Turkey*

[2]*Physics Division, Faculty of Arts and Sciences, Doğuş University Acıbadem-Kadıköy, 34722, Istanbul, Turkey*

(Received 1 January 2010; published 26 March 2010)

Taking into account the Λ baryon distribution amplitudes and the most general form of the interpolating current of the Λ_b, the semileptonic $\Lambda_b \to \Lambda \ell^+ \ell^-$ transition is investigated in the framework of the light cone QCD sum rules. Sum rules for all 12 form factors responsible for the $\Lambda_b \to \Lambda \ell^+ \ell^-$ decay are constructed. The obtained results for the form factors are used to compute the branching fraction. A comparison of the obtained results with the existing predictions of the heavy quark effective theory is presented. The results of the branching ratio shows the detectability of this channel at the Large Hadron Collider beauty in the near future is quite high.

DOI: 10.1103/PhysRevD.81.056006 PACS numbers: 11.55.Hx, 13.30.−a, 14.20.Mr

I. INTRODUCTION

Experimentally, the detection and isolation of the heavy baryons is simple compared to the light systems since having the heavy quark makes their beam narrow. In recent years, considerable experimental progress has been made in the identification and spectroscopy of the heavy baryons containing a heavy bottom or charm quark [1–8]. This evidence can be considered as a good signal to search also the decay channels of the heavy baryons such as $\Lambda_b \to \Lambda \ell^+ \ell^-$ at the LHCb. This rare channel, induced by the flavor changing neutral currents of $b \to s$ transition, serves as a testing ground for the standard model at loop level and is very sensitive to the new physics effects [9], such as supersymmetric particles [10], light dark matter [11]. and also the fourth generation of the quarks and extra dimensions, etc. Moreover, this channel can be inspected as a useful tool in the exact determination of the Cabibbo-Kobayashi-Maskawa matrix elements, V_{tb} and V_{ts}, CP and T violations, polarization asymmetries.

Theoretically, there are some works devoted to the analysis of the heavy baryon decays, where in practically all of them the predictions of the heavy quark effective theory (HQET) for form factors have been used. Transition form factors of the $\Lambda_b \to \Lambda_c$ and $\Lambda_c \to \Lambda$ decays have been studied in three point QCD sum rules in [12], the $\Lambda_b \to p l \nu$ transition form factors have also been calculated via three point QCD sum rules in the context of the HQET in [13] and in the framework of the SU(3) symmetry and HQET in [14]. In the present work, using the most general form of the interpolating current for the Λ_b and also the distribution amplitudes of Λ baryon, all form factors related to the electroweak penguin and weak box diagrams describing the $\Lambda_b \to \Lambda \ell^+ \ell^-$ are calculated in the framework of the light cone QCD sum rules in full theory. The obtained results for the form factors are used to estimate the decay rate and branching ratio. This transition has been investigated in [15,16] also in the context of the HQET but in the same framework using the distribution amplitudes of the Λ and Λ_b, respectively. Moreover, form factors, branching ratio, and dilepton forward-backward asymmetries are studied in [17–19] also within the context of the HQET. In [20–22], $\Sigma_{b,c}$ and $\Lambda_{b,c}$ to nucleon transitions are also evaluated using the nucleon wave functions in the light cone QCD sum rules approach.

The plan of the paper is as follows: in Sec. II, the light cone QCD sum rules for the form factors are obtained using the Λ distribution amplitudes (DA's). The HQET relations among all form factors are also discussed in this section. Section III is dedicated to the numerical analysis of the sum rules for the form factors as well as numerical results of the decay rate and branching ratio.

II. THEORETICAL FRAMEWORK

The $\Lambda_b \to \Lambda \ell^+ \ell^-$ channel proceeds via flavor changing neutral currents $b \to s$ transition at quark level. The effective Hamiltonian describing the electroweak penguin and weak box diagrams related to this transition can be written as

$$\mathcal{H}_{\text{eff}} = \frac{G_F \alpha_{em} V_{tb} V_{ts}^*}{2\sqrt{2}\pi} \Big\{ C_9^{\text{eff}} \bar{s} \gamma_\mu (1 - \gamma_5) b \bar{l} \gamma^\mu l + C_{10} \bar{s} \gamma_\mu (1 - \gamma_5) b \bar{l} \gamma^\mu \gamma_5 l - 2 m_b C_7 \frac{1}{q^2} \bar{s} i \sigma_{\mu\nu} q^\nu (1 + \gamma_5) b \bar{l} \gamma^\mu l \Big\}. \quad (1)$$

To find the amplitude, we need to sandwich this effective Hamiltonian between the initial and final baryon states, i.e., $\langle \Lambda_b(p+q) | \mathcal{H}_{\text{eff}} | \Lambda(p) \rangle$. From Eq. (1) we see that in

*taliev@metu.edu.tr
†Permanent address: Institute of Physics, Baku, Azerbaijan
‡kazizi@dogus.edu.tr
§savci@metu.edu.tr

the calculation of the $\Lambda_b \to \Lambda \ell^+ \ell^-$ decay amplitude, the matrix elements, $\langle \Lambda_b(p+q)|\bar{b}\gamma_\mu(1-\gamma_5)s|\Lambda(p)\rangle$ and $\langle \Lambda_b(p+q)|\bar{b}i\sigma_{\mu\nu}q^\nu(1+\gamma_5)s|\Lambda(p)\rangle$ appear. These matrix elements can be parametrized in terms of the 12 form factors, f_i, g_i, f_i^T, and g_i^T in the following manner:

$$\begin{aligned}\langle \Lambda(p)|\bar{s}\gamma_\mu(1-\gamma_5)b|\Lambda_b(p+q)\rangle &= \bar{u}_\Lambda(p)[\gamma_\mu f_1(Q^2) + i\sigma_{\mu\nu}q^\nu f_2(Q^2) + q^\mu f_3(Q^2) \\ &\quad - \gamma_\mu\gamma_5 g_1(Q^2) - i\sigma_{\mu\nu}\gamma_5 q^\nu g_2(Q^2) \\ &\quad - q^\mu\gamma_5 g_3(Q^2)]u_{\Lambda_b}(p+q), \end{aligned} \tag{2}$$

and

$$\begin{aligned}\langle \Lambda(p)|\bar{s}i\sigma_{\mu\nu}q^\nu(1+\gamma_5)b|\Lambda_b(p+q)\rangle &= \bar{u}_\Lambda(p)[\gamma_\mu f_1^T(Q^2) + i\sigma_{\mu\nu}q^\nu f_2^T(Q^2) + q^\mu f_3^T(Q^2) \\ &\quad + \gamma_\mu\gamma_5 g_1^T(Q^2) + i\sigma_{\mu\nu}\gamma_5 q^\nu g_2^T(Q^2) \\ &\quad + q^\mu\gamma_5 g_3^T(Q^2)]u_{\Lambda_b}(p+q), \end{aligned} \tag{3}$$

where $Q^2 = -q^2$. For calculation of these form factors we use the QCD sum rules approach. To obtain the sum rules for the form factors in this approach, the following correlation functions, the main objects in this approach, are considered:

$$\begin{aligned}\Pi_\mu^I(p,q) &= i\int d^4x e^{-iqx}\langle 0|T\{J^{\Lambda_b}(0), \bar{b}(x)\gamma_\mu(1-\gamma_5)s(x))\}|\Lambda(p)\rangle, \\ \Pi_\mu^{II}(p,q) &= i\int d^4x e^{-iqx}\langle 0|T\{J^{\Lambda_b}(0), \bar{b}(x)i\sigma_{\mu\nu}q^\nu(1+\gamma_5)s(x)\}|\Lambda(p)\rangle, \end{aligned} \tag{4}$$

where, p represents the Λ's momentum and q is the transferred momentum and the J^{Λ_b} is interpolating current of Λ_b. The most general form of the interpolating current of Λ_b baryon can be written as

$$\begin{aligned}J^{\Lambda_b}(x) = \frac{1}{\sqrt{6}}\epsilon_{abc}\{2[(q_1^{aT}(x)Cq_2^b(x))\gamma_5 b^c(x) + \beta(q_1^{aT}(x)C\gamma_5 q_2^b(x))b^c(x)] + (q_1^{aT}(x)Cb^b(x))\gamma_5 q_2^c(x) \\ + \beta(q_1^{aT}(x)C\gamma_5 b^b(x))q_2^c(x) + (b^{aT}(x)Cq_2^b(x))\gamma_5 q_1^c(x) + \beta(b^{aT}(x)C\gamma_5 q_2^b(x))q_1^c(x)\}, \end{aligned} \tag{5}$$

where q_1 and q_2 are the u and d quarks, respectively, a, b, and c are color indexes, and C is the charge conjugation operator. The β is an arbitrary parameter with $\beta = -1$ corresponding to the Ioffe current.

In order to obtain the sum rules for the transition form factors, we will calculate the aforementioned correlation functions in two different ways, namely, physical (phenomenological) and theoretical (QCD) sides and equate these two representations isolating the ground state through the dispersion relation. Finally, to suppress the contribution of the higher states and continuum, we will apply the Borel transformation and continuum subtraction to both sides of the correlation function and impose the quark hadron duality assumption.

The first step is to calculate the physical side of the correlation functions. Saturating the correlation functions with complete set of the intermediate states with the same quantum numbers as the initial state, for the physical part of the correlation function we obtain,

$$\Pi_\mu^I(p,q) = \sum_s \frac{\langle 0|J^{\Lambda_b}(0)|\Lambda_b(p+q,s)\rangle\langle \Lambda_b(p+q,s)|\bar{b}\gamma_\mu(1-\gamma_5)s|\Lambda(p)\rangle}{m_{\Lambda_b}^2 - (p+q)^2} + \cdots, \tag{6}$$

$$\Pi_\mu^{II}(p,q) = \sum_s \frac{\langle 0|J^{\Lambda_b}(0)|\Lambda_b(p+q,s)\rangle\langle \Lambda_b(p+q,s)|\bar{b}i\sigma_{\mu\nu}q^\nu(1+\gamma_5)s|\Lambda(p)\rangle}{m_{\Lambda_b}^2 - (p+q)^2} + \cdots, \tag{7}$$

where the dots $\cdots$ represent the contribution of the higher states and continuum. The vacuum to the baryon matrix element of the interpolating current, $\langle 0|J^{\Lambda_b}(0)|\Lambda_b(p+q,s)\rangle$ is written in terms of the residue, λ_{Λ_b} as

$$\langle 0|J^{\Lambda_b}(0)|\Lambda_b(p+q,s)\rangle = \lambda_{\Lambda_Q}\bar{u}_{\Lambda_Q}(p+q,s). \tag{8}$$

Putting Eqs. (2), (3), and (8) in Eqs. (6) and (7) and performing summation over spins of the Λ_b baryon using

$$\sum_s u_{\Lambda_b}(p+q,s)\bar{u}_{\Lambda_b}(p+q,s) = \not{p} + \not{q} + m_{\Lambda_b}, \tag{9}$$

we get the following expressions for the correlation functions:

$$\begin{aligned}\Pi_\mu^I(p,q) = \lambda_{\Lambda_b}\frac{\not{p}+\not{q}+m_{\Lambda_b}}{m_{\Lambda_b}^2-(p+q)^2}\{\gamma_\mu f_1 - i\sigma_{\mu\nu}q^\nu f_2 \\ + q_\mu f_3 - \gamma_\mu\gamma_5 g_1 - i\sigma_{\mu\nu}q^\nu\gamma_5 g_2 \\ + q_\mu\gamma_5 g_3\}u_\Lambda(p), \end{aligned} \tag{10}$$

$$\Pi^{II}_{\mu}(p,q)=\lambda_{\Lambda_b}\frac{\not p+\not q+m_{\Lambda_b}}{m^2_{\Lambda_b}-(p+q)^2}\{\gamma_\mu f_1^T-i\sigma_{\mu\nu}q^\nu f_2^T+q^\mu f_3^T+\gamma_\mu\gamma_5 g_1^T+i\sigma_{\mu\nu}\gamma_5 q^\nu g_2^T-q^\mu\gamma_5 g_3^T\}u_\Lambda(p). \quad (11)$$

Using the equation of motion and Eqs. (10) and (11), we get the following final expressions for the phenomenological sides of the correlation functions:

$$\Pi^{I}_{\mu}(p,q)=\frac{\lambda_{\Lambda_b}}{m^2_{\Lambda_b}-(p+q)^2}\{2f_1(Q^2)p_\mu+2f_2(Q^2)p_\mu\not q+[f_2(Q^2)+f_3(Q^2)]q_\mu\not q-2g_1(Q^2)p_\mu\gamma_5+2g_2(Q^2)p_\mu\not q\gamma_5+[g_2(Q^2)+g_3(Q^2)]q_\mu\not q\gamma_5+\text{other structures}\}u_\Lambda(p), \quad (12)$$

$$\Pi^{II}_{\mu}(p,q)=\frac{\lambda_{\Lambda_b}}{m^2_{\Lambda_b}-(p+q)^2}\{2f_1^T(Q^2)p_\mu+2f_2^T(Q^2)p_\mu\not q+[f_2^T(Q^2)+f_3^T(Q^2)]q_\mu\not q+2g_1^T(Q^2)p_\mu\gamma_5-2g_2^T(Q^2)p_\mu\not q\gamma_5-[g_2^T(Q^2)+g_3^T(Q^2)]q_\mu\not q\gamma_5+\text{other structures}\}u_\Lambda(p). \quad (13)$$

To compute the form factors or their combinations, f_1, f_2, f_2+f_3, g_1, g_2, and g_2+g_3, we will choose the independent structures p_μ, $p_\mu\not q$, $q_\mu\not q$, $p_\mu\gamma_5$, $p_\mu\not q\gamma_5$, and $q_\mu\not q\gamma_5$ from Eq. (12), respectively. The same structures are selected to calculate the form factors or their combinations labeled by T in the second correlation function, Eq. (13).

The next step is to calculate the correlation functions from the QCD side in the deep Euclidean region where $(p+q)^2\ll 0$. To this aim, we expend the time ordering products of the interpolating current of the Λ_b and transition currents in the correlation functions [see Eq. (4)] near the light cone, $x^2\simeq 0$ via operator product expansion, where the short and long distance effects are separated. The former is calculated using the QCD perturbation theory, whereas the latter are parameterized in terms of the Λ DA's. Mathematically, this is equivalent to contract out all quark pairs in the time ordering product of the J^{Λ_b} and transition currents via the Wick's theorem. As a result of this procedure, we obtain the following representations of the correlation functions in the QCD side:

$$\Pi^{I}_{\mu}=\frac{-i}{\sqrt{6}}\epsilon^{abc}\int d^4x e^{iqx}\{[2(C)_{\eta\phi}(\gamma_5)_{\rho\beta}+(C)_{\eta\beta}(\gamma_5)_{\rho\phi}+(C)_{\beta\phi}(\gamma_5)_{\eta\rho}]+\beta[2(C\gamma_5)_{\eta\phi}(I)_{\rho\beta}+(C\gamma_5)_{\eta\beta}(I)_{\rho\phi}+(C\gamma_5)_{\beta\phi}(I)_{\eta\rho}]\}[\gamma_\mu(1-\gamma_5)]_{\sigma\theta}\times S_b(-x)_{\beta\sigma}\langle 0|u^a_\eta(0)s^b_\theta(x)d^c_\phi(0)|\Lambda(p)\rangle, \quad (14)$$

$$\Pi^{II}_{\mu}=\frac{-i}{\sqrt{6}}\epsilon^{abc}\int d^4x e^{iqx}\{[2(C)_{\eta\phi}(\gamma_5)_{\rho\beta}+(C)_{\eta\beta}(\gamma_5)_{\rho\phi}+(C)_{\beta\phi}(\gamma_5)_{\eta\rho}]+\beta[2(C\gamma_5)_{\eta\phi}(I)_{\rho\beta}+(C\gamma_5)_{\eta\beta}(I)_{\rho\phi}+(C\gamma_5)_{\beta\phi}(I)_{\eta\rho}]\}[iq^\nu\sigma_{\mu\nu}(1+\gamma_5)]_{\sigma\theta}\times S_b(-x)_{\beta\sigma}\langle 0|u^a_\eta(0)s^b_\theta(x)d^c_\phi(0)|\Lambda(p)\rangle. \quad (15)$$

The heavy quark propagator, $S_b(x)$ is calculated in [23]

$$S_b(x)=S_b^{\text{free}}(x)-ig_s\int\frac{d^4k}{(2\pi)^4}e^{-ikx}\times\int_0^1 dv\Big[\frac{\not k+m_Q}{(m_Q^2-k^2)^2}G^{\mu\nu}(vx)\sigma_{\mu\nu}+\frac{1}{m_Q^2-k^2}vx_\mu G^{\mu\nu}\gamma_\nu\Big], \quad (16)$$

where

$$S_b^{\text{free}}=\frac{m_b^2}{4\pi^2}\frac{K_1(m_b\sqrt{-x^2})}{\sqrt{-x^2}}-i\frac{m_b^2\not x}{4\pi^2x^2}K_2(m_b\sqrt{-x^2}) \quad (17)$$

and K_i are the Bessel functions. The terms proportional to the gluon field strength are contributed mainly to the four and five particle distribution functions [23–27] and are expected to be very small in our case; hence, when doing calculations, these terms are ignored. The matrix element $\epsilon^{abc}\langle 0|u^a_\eta(0)d^b_\theta(0)s^c_\phi(x)|\Lambda(p)\rangle$ appearing in Eqs. (14) and (15) represents the Λ's wave functions, which are calculated in [27], and we list them out for the completeness of this paper in the Appendix. Using the Λ wave functions and the expression of the heavy quark propagator, and after performing the Fourier transformation, the final expressions of the correlation functions for both vertexes are found in terms of the Λ DA's in the QCD or theoretical side.

In order to obtain the sum rules for the form factors, f_1, f_2, f_3, g_1, g_2, g_3, f_1^T, f_2^T, f_3^T, g_1^T, g_2^T, and g_3^T, we equate the coefficients of the corresponding structures from both sides of the correlation functions through the dispersion relations and apply Borel transformation with respect to $(p+q)^2$ to suppress the contribution of the higher states and continuum. The expressions for the sum rules of the form factors are very lengthy, so we will give only extrapolation formulas to explore their dependency on the transferred momentum squared q^2.

The explicit expressions of the sum rules for the form factors depict that to calculate the values of the form factors, we need also the expression of the residue, λ_{Λ_b}. This residue is calculated in [28].

A few words about the relations among the form factors in HQET are in order. In HQET, the number of independent form factors is reduced to two, F_1 and F_2, so the transition matrix element can be parameterized in terms of these two form factors as [28,29]

$$\langle \Lambda(p)|\bar{s}\Gamma b|\Lambda_b(p+q)\rangle = \bar{u}_\Lambda(p)[F_1(Q^2) + \not{v} F_2(Q^2)]\Gamma u_{\Lambda_b}(p+q). \quad (18)$$

Here, Γ refers to any Dirac matrices and $\not{v} = (\not{p} + \not{q})/m_{\Lambda_b}$. Comparing this matrix element with definitions of the form factors in Eqs. (2) and (3), the following relations among the form factors are obtained (see also [30,31]):

$$f_1 = g_1 = f_2^T = g_2^T = F_1 + \frac{m_\Lambda}{m_{\Lambda_b}} F_2,$$
$$f_2 = g_2 = f_3 = g_3 = \frac{F_2}{m_{\Lambda_b}}, \qquad f_1^T = g_1^T = \frac{F_2}{m_{\Lambda_b}} q^2,$$
$$f_3^T = -\frac{F_2}{m_{\Lambda_b}}(m_{\Lambda_b} - m_\Lambda), \qquad g_3^T = \frac{F_2}{m_{\Lambda_b}}(m_{\Lambda_b} + m_\Lambda). \quad (19)$$

III. NUMERICAL ANALYSIS

This section is devoted to the numerical analysis of the form factors, their extrapolation in terms of the momentum transferred square and calculation of the total decay rate and branching ratio for rare $\Lambda_b \to \Lambda \ell^+ \ell^-$ transition in QCD.

Some input parameters used in the numerical calculations are $\langle \bar{u}u\rangle(1\ \text{GeV}) = \langle \bar{d}d\rangle(1\ \text{GeV}) = -(0.243 \pm 0.01)^3\ \text{GeV}^3$, $m_0^2(1\ \text{GeV}) = (0.8 \pm 0.2)\ \text{GeV}^2$ [32], $m_\Lambda = (1115.683 \pm 0.006)$ MeV, $m_{\Lambda_b} = (5620.2 \pm 1.6)$ MeV and $m_b = (4.7 \pm 0.1)$ GeV. Sum rules for the form factors depict that the Λ DA's are the main input parameters (see the Appendix). They contain four independent parameters, which are given as [27]

$$f_\Lambda = (6.0 \pm 0.3) \times 10^{-3}\ \text{GeV}^2,$$
$$\lambda_1 = (1.0 \pm 0.3) \times 10^{-2}\ \text{GeV}^2,$$
$$|\lambda_2| = (0.83 \pm 0.05) \times 10^{-2}\ \text{GeV}^2,$$
$$|\lambda_3| = (0.83 \pm 0.05) \times 10^{-2}\ \text{GeV}^2. \quad (20)$$

It is well known that, the Wilson coefficient C_9^{eff} receives long distance contributions from the J/ψ family, in addition to short distance contributions. In the present work, we do not take into account the long distance effects. From the explicit expressions for the form factors, it is clear that they depend on three auxiliary parameters, continuum threshold s_0, Borel mass parameter M_B^2, and the parameter β entering the most general form of the interpolating current of the Λ_b. The form factors should be independent of these auxiliary parameters. Therefore, we look for working regions for these parameters, where the form factors are practically independent of them. To determine the working region for the Borel mass parameter the procedure is as follows: the lower limit is obtained requiring that the higher states and continuum contributions constitute a small percentage of the total dispersion integral. The upper limit of M_B^2 is chosen demanding that the series of the light cone expansion with increasing twist should be convergent. As a result, the common working region of M_B^2 is found to be $15\ \text{GeV}^2 \le M_B^2 \le 30\ \text{GeV}^2$. As an example, we present the dependence of the form factor f_1 on the Borel mass parameter, M_B^2 at two fixed values of q^2 in Fig. 1. From this figure it follows that the form factor f_1 exhibits good stability with respect to the variations of M_B^2. The continuum threshold s_0 is correlated to the first exited state with quantum numbers of the interpolating current of the Λ_b and is not completely arbitrary. Numerical analysis leads to the interval, $(m_{\Lambda_b} + 0.3)^2 \le s_0 \le (m_{\Lambda_b} + 0.5)^2$, where the form factors weakly depend on the continuum threshold. In order to attain the working region for the parameter, β, we look for variation of the form factors with respect to $\cos\theta$, where $\beta = \tan\theta$. After performing numerical calculations, we obtained that in the interval $-0.6 \le \cos\theta \le 0.3$ all form factors weakly depend on β. As an example, we show the dependence of the form factor, f_1 on $\cos\theta$ at two fixed values of the q^2 and at $M_B^2 = 22\ \text{GeV}^2$ in Fig. 2. From this figure indeed we see that in the aforementioned region of $\cos\theta$, the form factor f_1 weakly depends on β.

The analysis of the sum rules, as has already been explained above, is based on the so-called standard procedure, i.e., the continuum threshold s_0 is independent of M_B^2 and q^2. However, in [33], instead of the standard procedure, namely, independence of the s_0 from M_B^2 and q^2, it is assumed that the continuum threshold depends on M_B^2 and q^2, and this leads to large realistic errors. Following [33], in the present work the systematic error is taken to be around 15%.

In calculating the branching ratio of the $\Lambda_b \to \Lambda \ell^+ \ell^-$ decay, the dependence of the form factors $f_i(q^2)$, $g_i(q^2)$, $f_i^T(q^2)$, and $g_i^T(q^2)$ on q^2 in the physical region $4m_\ell^2 \le q^2 \le (m_{\Lambda_b} - m_\Lambda)^2$ are needed. But unfortunately, sum rules predictions for the form factors are not reliable in the entire physical region. Therefore, in order to obtain the

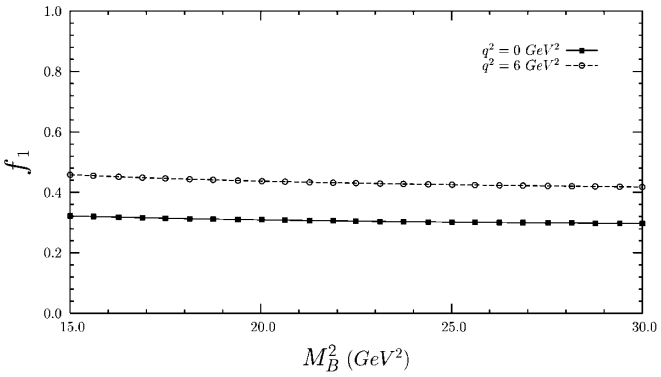

FIG. 1. The dependence of form factor f_1 on the Borel mass parameter at two fixed values of the q^2, and at $s_0 = 35\ \text{GeV}^2$ and $\beta = 5$.

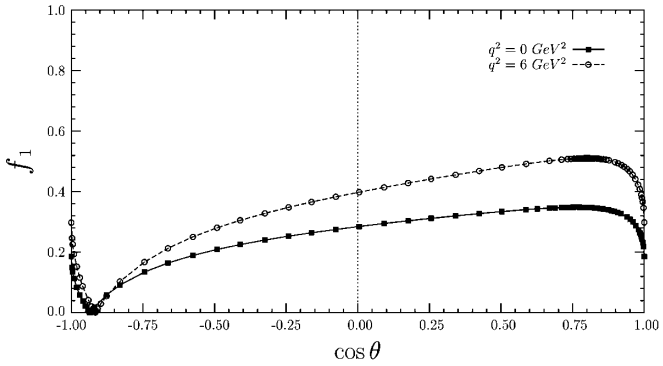

FIG. 2. The dependence of form factor f_1 on the $\cos\theta$ parameter at two fixed values of the q^2, and at $s_0 = 35$ GeV^2 and $M_B^2 = 22$ GeV^2.

q^2 dependence of the form factors from sum rules, we consider a range of q^2 where the correlation function can reliably be calculated. To this aim. we choose a region that is approximately 1 GeV below the perturbative cut, i.e., up to $q^2 \simeq 12$ GeV^2. To be able to extend the results for the form factors to the whole physical region, we look for a parameterization of the form factors in such a way that in the region $4m_\ell^2 \leq q^2 \leq 12$ GeV^2 this parameterization coincides with the sum rules predictions.

The next step is to present the q^2 dependency of the form factors. Our numerical calculations show that the best parameterization for the dependence of the form factors $f_1, f_2, f_3, g_1, g_2, g_3, f_2^T, f_3^T, g_2^T$, and g_3^T on q^2 is as follows:

$$f_i(q^2)[g_i(q^2)] = \frac{a}{(1-\frac{q^2}{m_{\rm fit}^2})} + \frac{b}{(1-\frac{q^2}{m_{\rm fit}^2})^2}, \qquad (21)$$

where the fit parameters a, b, and $m_{\rm fit}^2$ in full theory are given in Table I. On the other hand, we find that the best fit for the form factors f_1^T and g_1^T is of the following form:

TABLE I. Parameters appearing in the fit function of the form factors $f_1, f_2, f_3, g_1, g_2, g_3, f_2^T, f_3^T, g_2^T$, and g_3^T in full theory for $\Lambda_b \to \Lambda\ell^+\ell^-$. In this table, only central values of the parameters are presented.

	QCD sum rules		
	a	b	$m_{\rm fit}^2$
f_1	−0.046	0.368	39.10
f_2	0.046	−0.017	26.37
f_3	0.006	−0.021	22.99
g_1	−0.220	0.538	48.70
g_2	0.005	−0.018	26.93
g_3	0.035	−0.050	24.26
f_2^T	−0.131	0.426	45.70
f_3^T	−0.046	0.102	28.31
g_2^T	−0.369	0.664	59.37
g_3^T	−0.026	−0.075	23.73

TABLE II. Parameters appearing in the fit function of the form factors f_1^T and g_1^T in full theory for $\Lambda_b \to \Lambda\ell^+\ell^-$.

	QCD sum rules		
	c	$m_{\rm fit}^{\prime 2}$	$m_{\rm fit}^{\prime\prime 2}$
f_1^T	−1.191	23.81	59.96
g_1^T	−0.653	24.15	48.52

$$f_1^T(q^2)[g_1^T(q^2)] = \frac{c}{(1-\frac{q^2}{m_{\rm fit}^{\prime 2}})} - \frac{c}{(1-\frac{q^2}{m_{\rm fit}^{\prime\prime 2}})^2}. \qquad (22)$$

The results for the parameters c, $m_{\rm fit}^{\prime 2}$, and $m_{\rm fit}^{\prime\prime 2}$ are presented in Table II. In the extraction of the values of the fit parameters presented in both Tables I and II, the values of the continuum threshold $s_0 = 35$ GeV^2, Borel mass parameter $M_B^2 = 22$ GeV^2, and $\cos\theta = 0.2$ have been used.

The values of form factors at $q^2 = 0$ are also presented in Table III. In this table we also present the numerical results obtained from HQET, using the values for the form factors $F_1(0) = 0.462$ and $F_2 = -0.077$ predicted in [17], and relations in Eq. (19) at the HQET limit. The errors in the values of the form factors at $q^2 = 0$ are due to the uncertainties coming from M_B^2, s_0, the parameter β, errors in the input parameters, as well as from the systematic errors. From this table we see that, the predictions of the HQET on the form factors are changed more than 40% for the form factors $f_1(0)$, $g_1(0)$, $f_2^T(0)$, and $g_1^T(0)$, while the results of both approaches are very close to each other for the remaining form factors.

The final task is to calculate the total decay rate of the $\Lambda_b \to \Lambda\ell^+\ell^-$ transition in the whole physical region, $4m_\ell^2 \leq q^2 \leq (m_{\Lambda_b} - m_\Lambda)^2$. The differential decay rate is obtained as

$$\frac{d\Gamma}{ds} = \frac{G^2\alpha_{em}^2 m_{\Lambda_b}}{8192\pi^5}|V_{tb}V_{ts}^*|^2 v\sqrt{\lambda}\left[\Theta(s) + \frac{1}{3}\Delta(s)\right], \qquad (23)$$

TABLE III. The values of the form factors at $q^2 = 0$ for $\Lambda_b \to \Lambda\ell^+\ell^-$.

	Present work	HQET ([13])
$f_1(0)$	0.322 ± 0.112	0.446
$f_2(0)$	-0.011 ± 0.004	−0.013
$f_3(0)$	-0.015 ± 0.005	−0.013
$g_1(0)$	0.318 ± 0.110	0.446
$g_2(0)$	-0.013 ± 0.004	−0.013
$g_3(0)$	-0.014 ± 0.005	−0.013
$f_1^T(0)$	0 ± 0.0	0.0
$f_2^T(0)$	0.295 ± 0.105	0.446
$f_3^T(0)$	0.056 ± 0.018	0.061
$g_1^T(0)$	0 ± 0.0	0.0
$g_2^T(0)$	0.294 ± 0.105	0.446
$g_3^T(0)$	-0.101 ± 0.035	−0.092

where $s = q^2/m_{\Lambda_b}^2$, $r = m_\Lambda^2/m_{\Lambda_b}^2$, $\lambda = \lambda(1, r, s) = 1 + r^2 + s^2 - 2r - 2s - 2rs$, $G_F = 1.17 \times 10^{-5}$ GeV^{-2} is the Fermi coupling constant, and $\upsilon = \sqrt{1 - \frac{4m_\ell^2}{q^2}}$ is the lepton velocity. For the element of the Cabibbo-Kobayashi-Maskawa matrix $|V_{tb}V_{ts}^*| = 0.041$ has been used [34]. The functions $\Theta(s)$ and $\Delta(s)$ are given as

$$\begin{aligned}\Theta(s) &= 32m_\ell^2 m_{\Lambda_b}^4 s(1 + r - s)(|D_3|^2 + |E_3|^2) + 64m_\ell^2 m_{\Lambda_b}^3(1 - r - s)\,\mathrm{Re}[D_1^* E_3 + D_3 E_1^*] \\ &+ 64m_{\Lambda_b}^2\sqrt{r}(6m_\ell^2 - m_{\Lambda_b}^2 s)\,\mathrm{Re}[D_1^* E_1] + 64m_\ell^2 m_{\Lambda_b}^3\sqrt{r}(2m_{\Lambda_b} s\,\mathrm{Re}[D_3^* E_3] + (1 - r + s)\,\mathrm{Re}[D_1^* D_3 + E_1^* E_3]) \\ &+ 32m_{\Lambda_b}^2(2m_\ell^2 + m_{\Lambda_b}^2 s)\{(1 - r + s)m_{\Lambda_b}\sqrt{r}\,\mathrm{Re}[A_1^* A_2 + B_1^* B_2] - m_{\Lambda_b}(1 - r - s)\,\mathrm{Re}[A_1^* B_2 + A_2^* B_1] \\ &- 2\sqrt{r}(\mathrm{Re}[A_1^* B_1] + m_{\Lambda_b}^2 s\,\mathrm{Re}[A_2^* B_2])\} + 8m_{\Lambda_b}^2\{4m_\ell^2(1 + r - s) + m_{\Lambda_b}^2[(1 - r)^2 - s^2]\}(|A_1|^2 + |B_1|^2) \\ &+ 8m_{\Lambda_b}^4\{4m_\ell^2[\lambda + (1 + r - s)s] + m_{\Lambda_b}^2 s[(1 - r)^2 - s^2]\}(|A_2|^2 + |B_2|^2) - 8m_{\Lambda_b}^2\{4m_\ell^2(1 + r - s) \\ &- m_{\Lambda_b}^2[(1 - r)^2 - s^2]\}(|D_1|^2 + |E_1|^2) + 8m_{\Lambda_b}^5 s\upsilon^2\{-8m_{\Lambda_b} s\sqrt{r}\,\mathrm{Re}[D_2^* E_2] + 4(1 - r + s)\sqrt{r}\,\mathrm{Re}[D_1^* D_2 + E_1^* E_2] \\ &- 4(1 - r - s)\,\mathrm{Re}[D_1^* E_2 + D_2^* E_1] + m_{\Lambda_b}[(1 - r)^2 - s^2](|D_2|^2 + |E_2|^2)\}, \end{aligned} \tag{24}$$

$$\Delta(s) = -8m_{\Lambda_b}^4\upsilon^2\lambda(|A_1|^2 + |B_1|^2 + |D_1|^2 + |E_1|^2) + 8m_{\Lambda_b}^6 s\upsilon^2\lambda(|A_2|^2 + |B_2|^2 + |D_2|^2 + |E_2|^2), \tag{25}$$

where

$$\begin{aligned} A_1 &= \frac{1}{q^2}(f_1^T + g_1^T)(-2m_b C_7) + (f_1 - g_1)C_9^{\mathrm{eff}} \\ A_2 &= A_1(1 \to 2), \qquad A_3 = A_1(1 \to 3), \\ B_1 &= A_1(g_1 \to -g_1; g_1^T \to -g_1^T), \qquad B_2 = B_1(1 \to 2), \\ B_3 &= B_1(1 \to 3), \\ D_1 &= (f_1 - g_1)C_{10}, \qquad D_2 = D_1(1 \to 2), \end{aligned} \tag{26}$$

$$\begin{aligned} D_3 &= D_1(1 \to 3), \qquad E_1 = D_1(g_1 \to -g_1), \\ E_2 &= E_1(1 \to 2), \qquad E_3 = E_1(1 \to 3). \end{aligned} \tag{27}$$

Integrating the differential decay rate on s in the entire physical region $4m_\ell^2/m_{\Lambda_b}^2 \le s \le (1 - \sqrt{r})^2$ and using the lifetime of the Λ_b baryon, $\tau_{\Lambda_b} = 1.383 \times 10^{-12} s$ [34], we obtain the results for the branching ratio, which are presented in Table IV.

In this table we also present the values of the branching ratio obtained in HQET [19]. Comparing the results of both approaches, we see that our predictions on the branching ratios for the $\Lambda_b \to \Lambda e^+ e^-$, $\Lambda_b \to \Lambda \mu^+ \mu^-$ channels are larger than the ones predicted by the HQET approximately by a factor of 2, while for the $\Lambda_b \to \Lambda \tau^+ \tau^-$ channel our prediction is 4 times larger than the result of the HQET. Since $10^{10} \div 10^{11}$ pairs are expected to be produced per year at the LHCb [35], the results presented in Table IV show that detectability of $\Lambda_b \to \Lambda \ell^+ \ell^- (\ell = e, \mu, \tau)$ decays in this machine is quite high.

In conclusion, we calculate all 12 form factors responsible for the $\Lambda_b \to \Lambda \ell^+ \ell^-$ decay within light cone sum rules. The maximum difference between our results and the HQET predictions on the form factors is about 40%. Using the parametrization for the form factors, the branching ratio of the $\Lambda_b \to \Lambda \ell^+ \ell^-$ decay is estimated, and the result we obtain allows us to conclude that the delectability of this decay at the LHCb is quite high.

APPENDIX

In this Appendix, the general decomposition of the matrix element, $\epsilon^{abc}\langle 0|u_\eta^a(0)s_\theta^b(x)d_\phi^c(0)|\Lambda(p)\rangle$ entering Eqs. (14) and (15) as well as the Λ DA's are given [27]:

TABLE IV. Values of the branching ratio for $\Lambda_b \to \Lambda \ell^+ \ell^-$ in full theory and HQET for different leptons.

	Present work	HQET ([19])
$\mathrm{Br}(\Lambda_b \to \Lambda e^+ e^-)$	$(4.6 \pm 1.6) \times 10^{-6}$	$(2.23 \div 3.34) \times 10^{-6}$
$\mathrm{Br}(\Lambda_b \to \Lambda \mu^+ \mu^-)$	$(4.0 \pm 1.2) \times 10^{-6}$	$(2.08 \div 3.19) \times 10^{-6}$
$\mathrm{Br}(\Lambda_b \to \Lambda \tau^+ \tau^-)$	$(0.8 \pm 0.3) \times 10^{-6}$	$(0.179 \div 0.276) \times 10^{-6}$

$$
\begin{aligned}
&4\langle 0|\epsilon^{abc}u^a_\alpha(a_1x)s^b_\beta(a_2x)d^c_\gamma(a_3x)|\Lambda(p)\rangle \\
&= \mathcal{S}_1 m_\Lambda C_{\alpha\beta}(\gamma_5\Lambda)_\gamma + \mathcal{S}_2 m^2_\Lambda C_{\alpha\beta}(\not{x}\gamma_5\Lambda)_\gamma + \mathcal{P}_1 m_\Lambda(\gamma_5 C)_{\alpha\beta}\Lambda_\gamma + \mathcal{P}_2 m^2_\Lambda(\gamma_5 C)_{\alpha\beta}(\not{x}\Lambda)_\gamma \\
&\quad + \left(\mathcal{V}_1 + \frac{x^2 m^2_\Lambda}{4}\mathcal{V}^M_1\right)(\not{p}C)_{\alpha\beta}(\gamma_5\Lambda)_\gamma + \mathcal{V}_2 m_\Lambda(\not{p}C)_{\alpha\beta}(\not{x}\gamma_5\Lambda)_\gamma + \mathcal{V}_3 m_\Lambda(\gamma_\mu C)_{\alpha\beta}(\gamma^\mu\gamma_5\Lambda)_\gamma \\
&\quad + \mathcal{V}_4 m^2_\Lambda(\not{x}C)_{\alpha\beta}(\gamma_5\Lambda)_\gamma + \mathcal{V}_5 m^2_\Lambda(\gamma_\mu C)_{\alpha\beta}(i\sigma^{\mu\nu}x_\nu\gamma_5\Lambda)_\gamma + \mathcal{V}_6 m^3_\Lambda(\not{x}C)_{\alpha\beta}(\not{x}\gamma_5\Lambda)_\gamma \\
&\quad + \left(\mathcal{A}_1 + \frac{x^2 m^2_\Lambda}{4}\mathcal{A}^M_1\right)(\not{p}\gamma_5 C)_{\alpha\beta}\Lambda_\gamma + \mathcal{A}_2 m_\Lambda(\not{p}\gamma_5 C)_{\alpha\beta}(\not{x}\Lambda)_\gamma + \mathcal{A}_3 m_\Lambda(\gamma_\mu\gamma_5 C)_{\alpha\beta}(\gamma^\mu\Lambda)_\gamma + \mathcal{A}_4 m^2_\Lambda(\not{x}\gamma_5 C)_{\alpha\beta}\Lambda_\gamma \\
&\quad + \mathcal{A}_5 m^2_\Lambda(\gamma_\mu\gamma_5 C)_{\alpha\beta}(i\sigma^{\mu\nu}x_\nu\Lambda)_\gamma + \mathcal{A}_6 m^3_\Lambda(\not{x}\gamma_5 C)_{\alpha\beta}(\not{x}\Lambda)_\gamma + \left(\mathcal{T}_1 + \frac{x^2 m^2_\Lambda}{4}\mathcal{T}^M_1\right)(p^\nu i\sigma_{\mu\nu}C)_{\alpha\beta}(\gamma^\mu\gamma_5\Lambda)_\gamma \\
&\quad + \mathcal{T}_2 m_\Lambda(x^\mu p^\nu i\sigma_{\mu\nu}C)_{\alpha\beta}(\gamma_5\Lambda)_\gamma + \mathcal{T}_3 m_\Lambda(\sigma_{\mu\nu}C)_{\alpha\beta}(\sigma^{\mu\nu}\gamma_5\Lambda)_\gamma + \mathcal{T}_4 m_\Lambda(p^\nu\sigma_{\mu\nu}C)_{\alpha\beta}(\sigma^{\mu\rho}x_\rho\gamma_5\Lambda)_\gamma \\
&\quad + \mathcal{T}_5 m^2_\Lambda(x^\nu i\sigma_{\mu\nu}C)_{\alpha\beta}(\gamma^\mu\gamma_5\Lambda)_\gamma + \mathcal{T}_6 m^2_\Lambda(x^\mu p^\nu i\sigma_{\mu\nu}C)_{\alpha\beta}(\not{x}\gamma_5\Lambda)_\gamma + \mathcal{T}_7 m^2_\Lambda(\sigma_{\mu\nu}C)_{\alpha\beta}(\sigma^{\mu\nu}\not{x}\gamma_5\Lambda)_\gamma \\
&\quad + \mathcal{T}_8 m^3_\Lambda(x^\nu\sigma_{\mu\nu}C)_{\alpha\beta}(\sigma^{\mu\rho}x_\rho\gamma_5\Lambda)_\gamma. \qquad \text{(A1)}
\end{aligned}
$$

The calligraphic functions in the above expression do not have definite twists but they can be written in terms of the Lambda distribution amplitudes (DA's) with definite and increasing twists via the scalar product px and the parameters a_i, $i = 1, 2, 3$. The explicit expressions for scalar, pseudoscalar, vector, axial vector, and tensor DA's for Lambda are given in Tables V, VI, VII, VIII, and IX, respectively.

Every distribution amplitude $F(a_i px) = S_i$, P_i, V_i, A_i, T_i can be represented as

$$
F(a_i px) = \int dx_1 dx_2 dx_3 \delta(x_1 + x_2 + x_3 - 1) \times e^{ipx\Sigma_i x_i a_i} F(x_i), \qquad \text{(A2)}
$$

where x_i with $i = 1$, 2, and 3 are longitudinal momentum fractions carried by the participating quarks.

The explicit expressions for the Λ DA's up to twist 6 are given as twist-3 DA's:

$$
V_1(x_i) = 0, \qquad A_1(x_i) = -120x_1x_2x_3\phi^0_3, \qquad T_1(x_i) = 0. \qquad \text{(A3)}
$$

twist-4 DA's:

TABLE V. Relations between the calligraphic functions and Lambda scalar DA's.

$\mathcal{S}_1 = S_1$
$2px\mathcal{S}_2 = S_1 - S_2$

TABLE VI. Relations between the calligraphic functions and Lambda pseudoscalar DA's.

$\mathcal{P}_1 = P_1$
$2px\mathcal{P}_2 = P_1 - P_2$

TABLE VII. Relations between the calligraphic functions and Lambda vector DA's.

$\mathcal{V}_1 = V_1$
$2px\mathcal{V}_2 = V_1 - V_2 - V_3$
$2\mathcal{V}_3 = V_3$
$4px\mathcal{V}_4 = -2V_1 + V_3 + V_4 + 2V_5$
$4px\mathcal{V}_5 = V_4 - V_3$
$4(px)^2\mathcal{V}_6 = -V_1 + V_2 + V_3 + V_4 + V_5 - V_6$

TABLE VIII. Relations between the calligraphic functions and Lambda axial vector DA's.

$\mathcal{A}_1 = A_1$
$2px\mathcal{A}_2 = -A_1 + A_2 - A_3$
$2\mathcal{A}_3 = A_3$
$4px\mathcal{A}_4 = -2A_1 - A_3 - A_4 + 2A_5$
$4px\mathcal{A}_5 = A_3 - A_4$
$4(px)^2\mathcal{A}_6 = A_1 - A_2 + A_3 + A_4 - A_5 + A_6$

TABLE IX. Relations between the calligraphic functions and Lambda tensor DA's.

$\mathcal{T}_1 = T_1$
$2px\mathcal{T}_2 = T_1 + T_2 - 2T_3$
$2\mathcal{T}_3 = T_7$
$2px\mathcal{T}_4 = T_1 - T_2 - 2T_7$
$2px\mathcal{T}_5 = -T_1 + T_5 + 2T_8$
$4(px)^2\mathcal{T}_6 = 2T_2 - 2T_3 - 2T_4 + 2T_5 + 2T_7 + 2T_8$
$4px\mathcal{T}_7 = T_7 - T_8$
$4(px)^2\mathcal{T}_8 = -T_1 + T_2 + T_5 - T_6 + 2T_7 + 2T_8$

$$
\begin{aligned}
S_1(x_i) &= 6x_3(1-x_3)(\xi_4^0+\xi_4^{\prime 0}),\\
P_1(x_i) &= 6(1-x_3)(\xi_4^0-\xi_4^{\prime 0}),\\
V_2(x_i) &= 0,\\
A_2(x_i) &= -24x_1x_2\phi_4^0,\\
V_3(x_i) &= 12(x_1-x_2)x_3\psi_4^0,\\
A_3(x_i) &= -12x_3(1-x_3)\psi_4^0,\\
T_2(x_i) &= 0,\\
T_3(x_i) &= 6(x_2-x_1)x_3(-\xi_4^0+\xi_4^{\prime 0}),\\
T_7(x_i) &= -6(x_1-x_2)x_3(\xi_4^0+\xi_4^{\prime 0}).
\end{aligned}
\tag{A4}
$$

twist-5 DA's:

$$
\begin{aligned}
S_2(x_i) &= \tfrac{3}{2}(x_1+x_2)(\xi_5^0+\xi_5^{\prime 0}),\\
P_2(x_i) &= \tfrac{3}{2}(x_1+x_2)(\xi_5^0-\xi_5^{\prime 0}),\\
V_4(x_i) &= 3(x_2-x_1)\psi_5^0,\\
A_4(x_i) &= -3(1-x_3)\psi_5^0,\\
V_5(x_i) &= 0,\\
A_5(x_i) &= -6x_3\phi_5^0,\\
T_4(x_i) &= -\tfrac{3}{2}(x_1-x_2)(\xi_5^0+\xi_5^{\prime 0}),\\
T_5(x_i) &= 0,\\
T_8(x_i) &= -\tfrac{3}{2}(x_1-x_2)(\xi_5^0-\xi_5^{\prime 0}).
\end{aligned}
\tag{A5}
$$

and twist-6 DA's:

$$
V_6(x_i) = 0, \qquad A_6(x_i) = -2\phi_6^0, \qquad T_6(x_i) = 0. \tag{A6}
$$

The following functions are encountered to the above amplitudes, and they can be defined in terms of the four independent parameters, namely, f_Λ, λ_1, λ_2, and λ_3:

$$
\begin{aligned}
&\phi_3^0 = \phi_6^0 = -f_\Lambda, \qquad \phi_4^0 = \phi_5^0 = -\tfrac{1}{2}(f_\Lambda+\lambda_1),\\
&\psi_4^0 = \psi_5^0 = \tfrac{1}{2}(f_\Lambda-\lambda_1), \qquad \xi_4^0 = \xi_5^0 = \lambda_2+\lambda_3,\\
&\xi_4^{\prime 0} = \xi_5^{\prime 0} = \lambda_3-\lambda_2.
\end{aligned}
\tag{A7}
$$

[1] M. Mattson *et al.* (SELEX Collaboration), Phys. Rev. Lett. **89**, 112001 (2002).
[2] T. Aaltonen *et al.* (CDF Collaboration), Phys. Rev. Lett. **99**, 052002 (2007); **99**, 202001 (2007).
[3] R. Chistov *et al.* (Belle Collaboration), Phys. Rev. Lett. **97**, 162001 (2006).
[4] A. Ocherashvili *et al.* (SELEX Collaboration), Phys. Lett. B **628**, 18 (2005).
[5] V. Abazov *et al.* (D0 Collaboration), Phys. Rev. Lett. **99**, 052001 (2007); **101**, 232002 (2008).
[6] D. Acosta *et al.* (CDF Collaboration), Phys. Rev. Lett. **96**, 202001 (2006).
[7] B. Aubert *et al.* (*BABAR* Collaboration), Phys. Rev. Lett. **97**, 232001 (2006); **99**, 062001 (2007); Phys. Rev. D **77**, 012002 (2008).
[8] E. Solovieva *et al.* (Belle Collaboration), Phys. Lett. B **672**, 1 (2009).
[9] T. M. Aliev, A. Ozpineci, and M. Savci, Nucl. Phys. **B649**, 168 (2003).
[10] G. Buchalla, G. Hiller, and G. Isidori, Phys. Rev. D **63**, 014015 (2000).
[11] C. Bird, P. Jackson, R. Kowalewski, and M. Pospelov, Phys. Rev. Lett. **93**, 201803 (2004).
[12] R. S. Marques de Carvalho, F. S. Navarra, M. Nielsen, E. Ferreira, and H. G. Dosch, Phys. Rev. D **60**, 034009 (1999).
[13] C. -S. Huang, C. -F. Qiao, and H. -G. Yan, Phys. Lett. B **437**, 403 (1998).
[14] A. Datta, arXiv:hep-ph/9504429.
[15] Yu-Ming Wang, Ying Li, and Cai-Dian Lu, Eur. Phys. J. C **59**, 861 (2009).
[16] Yu-Ming Wang, Yue-Long Shen, and Cai-Dian Lu, Phys. Rev. D **80**, 074012 (2009).
[17] C. S. Huang and H. G. Yan, Phys. Rev. D **59**, 114022 (1999).
[18] C. -H. Chen and C. Q. Ceng, Phys. Lett. B **516**, 327 (2001).
[19] C. -H. Chen and C. Q. Ceng, Phys. Rev. D **64**, 074001 (2001).
[20] K. Azizi, M. Bayar, A. Ozpineci, and Y. Sarac, Phys. Rev. D **80**, 036007 (2009).
[21] K. Azizi, M. Bayar, Y. Sarac, and H. Sundu, Phys. Rev. D **80**, 096007 (2009).
[22] K. Azizi, M. Bayar, and M. T. Zeyrek, arXiv:0910.4521.
[23] I. I. Balitsky and V. M. Braun, Nucl. Phys. **B311**, 541 (1989).

[24] V. M. Braun, A. Lenz, N. Mahnke, and E. Stein, Phys. Rev. D **65**, 074011 (2002).
[25] V. M. Braun, A. Lenz, and M. Wittmann, Phys. Rev. D **73**, 094019 (2006); A. Lenz, M. Wittmann, and E. Stein, Phys. Lett. B **581**, 199 (2004).
[26] V. Braun, R. J. Fries, N. Mahnke, and E. Stein, Nucl. Phys. **B589**, 381 (2000).
[27] Y. L. Liu and M. Q. Huang, Nucl. Phys. **A821**, 80 (2009).
[28] T. M. Aliev, A. Ozpineci, and M. Savci, Phys. Rev. D **65**, 115002 (2002).
[29] T. Mannel, W. Roberts, and Z. Ryzak, Nucl. Phys. **B355**, 38 (1991).
[30] C. H. Chen and C. Q. Geng, Phys. Rev. D **63**, 054005 (2001); **63**, 114024 (2001); **64**, 074001 (2001).
[31] T. M. Aliev, A. Ozpineci, M. Savci, and C. Yuce, Phys. Lett. B **542**, 229 (2002).
[32] B. L. Ioffe, Prog. Part. Nucl. Phys. **56**, 232 (2006).
[33] W. Lucha, D. Melikhov, and S. Simula, Phys. Rev. D **79**, 096011 (2009).
[34] C. Amsler *et al.* (Particle Data Group), Phys. Lett. B **667**, 1 (2008).
[35] N. H. Harnew, *8th International Symposium on Heavy Flavour Physics, Southampton, UK, 1999*, (JHEP Proceedings, Trieste, Italy, 1999).